Application of the TranAir Full-Potential Code to the F-16A

L. L. Erickson,* M. D. Madson,* and A. C. Woo†
NASA Ames Research Center, Moffett Field, California

The TranAir computer code solves the full-potential equation for transonic flow by combining a rectangular box of flowfield grid points with networks of surface panels. Complex geometries are easily represented since surface-conforming flowfield grids are not used. Wing pressures predicted by TranAir are compared to wind-tunnel data at $\alpha = 4$ deg for $M_\infty = 0.6$ and 0.9. The higher Mach number condition produces supercritical flow and demonstrates TranAir's shock-capturing capability.

Introduction

THE major technical obstacle to routinely computing inviscid transonic flow about realistic aircraft "is the difficulty in generating suitable grids."[1] While it is difficult to produce flowfield grids that conform to the surface of complicated configurations, it is relatively easy to produce grids that are on the aircraft surface only. Such surface grids are used routinely by linear panel (boundary element) methods.

There has been recent progress in solving nonlinear fluid-flow problems by combining flowfield grid methods with surface-panel methods.[2-5] Such an approach is used in the TranAir computer code. TranAir combines portions of the surface-paneling technology from PanAir[6-9] with finite-element and optimization techniques to solve the conservative form of the full-potential equation. The basic approach is to embed surface panels in a rectangular box of grid points. The cells formed by the rectangular grid are used to discretize the full-potential equation with finite elements. The surface panels that slice through some of the finite-element cells alter the finite-element discretization in the vicinity of boundary surfaces. This approach enables transonic flow about very complex configurations to be computed without using a surface-conforming flowfield grid.

The present paper demonstrates this capability by comparing TranAir solutions with wind-tunnel data for the F-16A at freestream Mach numbers of $M_\infty = 0.6$ and 0.9 at $\alpha = 4$ deg. The TranAir model includes fuselage and canopy, engine nacelle (modeled with specified inlet-flow velocity), the diverter area between the nacelle inlet and the fuselage, wing and strake, ventral fins, vertical and horizontal stabilizers, and the cutouts between these stabilizers and the fuselage afterbody. These initial results are for the aircraft without wingtip missiles or underwing fuel tanks.

Methodology

The input quantities to TranAir are very similar to those of the PanAir linear-potential flow code. The aircraft surface is defined as a collection of abutting networks of surface grid points. Within each network, the surface grid points are used to define surface panels at which boundary conditions are specified. The most apparent input difference between the TranAir and PanAir codes is that a rectangular box of flowfield grid points must be defined for TranAir. If the user does not define the box explicitly, a default box is generated by the program. The paneled model is embedded in this rectangular grid, as shown in Fig. 1.

As in PanAir, each panel is subdivided into eight triangular subpanels to maintain geometric continuity between all panels within each network. The program checks all network edges for abutments with adjacent network edges. If unintended gaps are detected by the program they must be closed by the user, or the program can be instructed to change the coordinates of the intended abutting edges so that the gaps are eliminated.

Zero-thickness surfaces are also allowed. These are useful for simple models of lifting surfaces, e.g., struts and fins. In addition to defining the aircraft surface, special networks of wake panels are also used to enforce trailing-edge Kutta conditions.

User-specified boundary conditions can be imposed on either side of a nonwake panel. The program determines which points of the rectangular grid are exterior to, and interior to, the volume enclosed by the surface panels, and then uses the panel and rectangular grid-cell geometry to form finite-element relations between the boundary-condition data and the flowfield properties at the field grid points.

At the perimeter of the rectangular grid, the equation set being solved changes from the nonlinear full-potential equation to the linear Prandtl-Glauert equation. As a consequence, the rectangular computational grid need only encompass the nonlinear flow regions near the aircraft. The far-field boundary condition of zero potential at infinity is automatically satisfied by the discrete Green's function (for the Prandtl-Glauert equation) employed in the formulation. Consequently, the solution domain extends to infinity although the computational grid is finite, as indicated in Fig. 1.

The finite-element discretization yields a set of nonlinear algebraic equations, which are solved iteratively using an optimization algorithm called GMRES (Generalized Minimal Residual)[10] in conjunction with Newton linearization and multiple preconditioners. The preconditioning is achieved with 1) fast Fourier transforms (FFT) to evaluate convolution integrals involving the discrete Green's function, and 2) Gauss-Seidel incomplete iterations in one or more grid directions. The approximate solutions from the FFT and Gauss-Seidel operations for k iterations are saved, and then used by GMRES as search directions to obtain a much improved approximate solution. A value of $k = 20$ is typical. A more complete discussion of the theory is presented in Ref. 11.

TranAir Model of F-16A

The TranAir input model of the F-16A is shown in Fig. 2. The wing wake has been aligned with the angle of attack (4 deg). The one-panel-wide vertical wake connecting the wing and horizontal-stabilizer wakes is a constant-strength doublet network, which prevents the doublet strength on the inboard edge of the wing wake from being forced to zero (a condition

Received Oct. 2, 1986; revision received Feb. 21, 1987.

*Aerospace Engineer. Member AIAA.
†Research Scientist. Member AIAA.

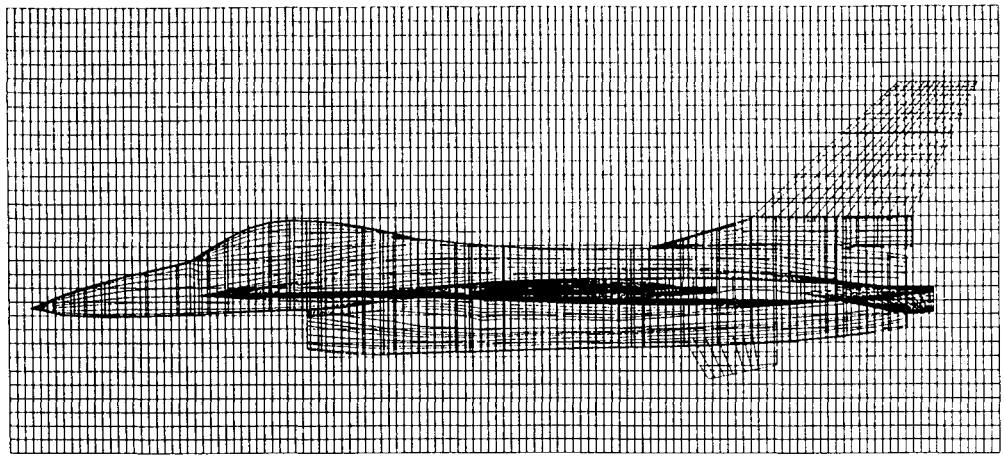

a) SIDE VIEW

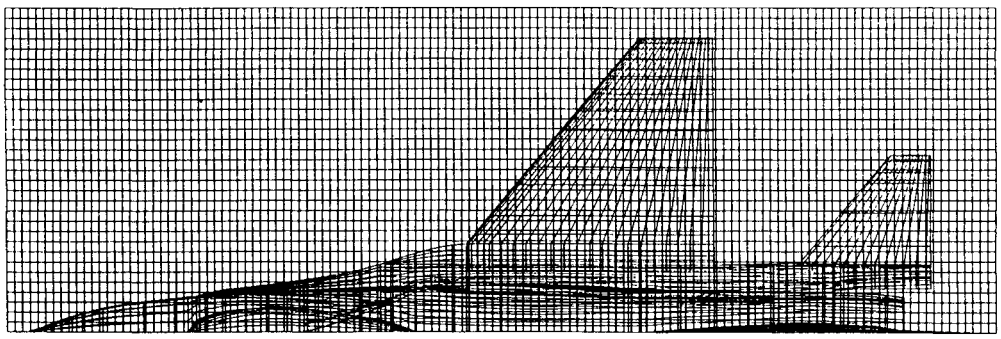

b) TOP VIEW

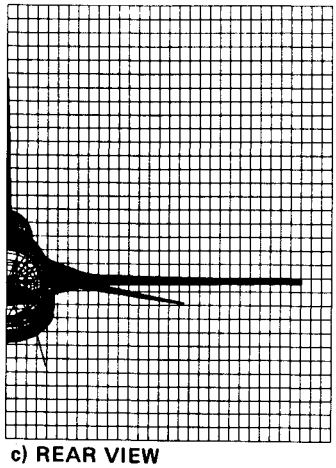

c) REAR VIEW

Fig. 1 Surface panels embedded in a box of $129 \times 33 \times 33$ rectangular-grid points.

that would cause an incorrect loss in wing circulation). For zero sideslip, the vertical stabilizer wake is omitted. TranAir wakes differ slightly from PanAir wakes. When a TranAir wake emerges from the downstream face of the rectangular box of flowfield grid points, the program terminates the rest of the wake beyond the grid box. The program then redefines the section of wake beyond the grid box to be parallel to the body axis. Thus, the wing wake on the TranAir model is parallel to the freestream until it reaches the aft end of the grid box, where it is modified by the program to run parallel to the body axis.

Only one-half of a symmetric configuration is required as input to the program. The right half of the F-16A is defined with 3185 surface panels, plus 252 wake panels. The right half of the rectangular grid box contains $129 \times 33 \times 33$ points in the x, y, and z directions, respectively. The grid spacing along each coordinate direction is uniform, but Δx, Δy, and Δz can each be different. Views of the paneled geometry of the F-16A are shown in Fig. 3. These views show several regions where the panel density is discontinuous, e.g., in the wing-strake/fuselage region where fewer chordwise panels are used on the fuselage than on the wing-strake.

In this initial model, the diverter geometry above the nacelle is included, but the nacelle inlet lip has been omitted. This omission was not due to any limitations within the program. The wind-tunnel model has a flowthrough duct connecting the inlet and afterbody regions. The TranAir model of the inlet face is a network of porous panels, on which the boundary conditions are 1) the velocity on the upstream side of the panels is the normal component of the freestream velocity, and 2) the perturbation potential on the downstream side of the panels is zero. The wing, strake, and vertical and horizontal stabilizers are modeled as thick surfaces (actual-surface geometry), with panels sealing the wing and stabilizer tips. For

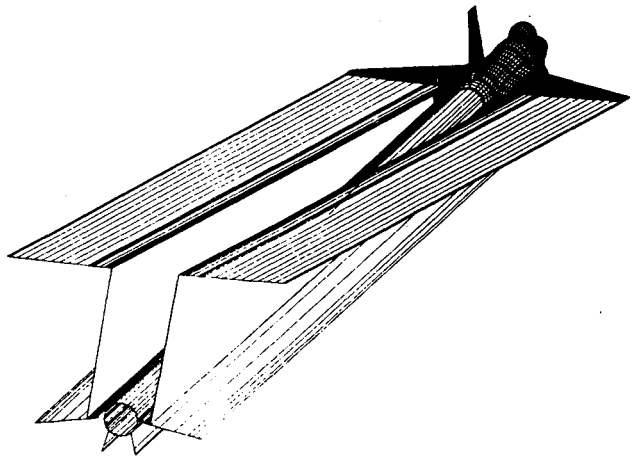

Fig. 2 Trailing wake networks.

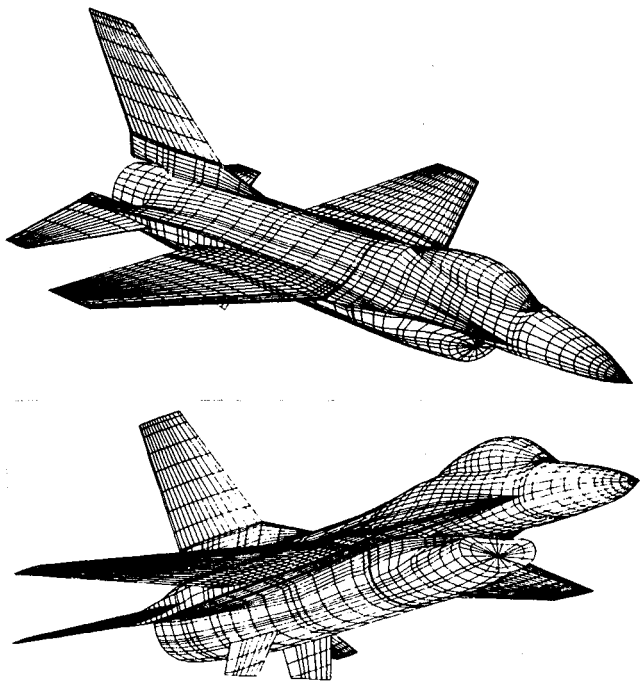

Fig. 3 Isometric views of surface paneling.

simplicity, and to show some of TranAir's modeling versatility, the ventral fin is approximated by a zero-thickness flat plate (mean-surface geometry).

The afterbody base is closed off with panels in the same manner as the inlet. The boundary conditions used on these base panels are 1) the total potential is constant on the downstream side, and 2) the perturbation potential is zero on the upstream side. The constant total potential on the downstream side, combined with the wake networks emanating from the afterbody perimeter (Fig. 2), cause the flow to separate smoothly from the afterbody trailing edge, i.e., the flow does not turn through a right angle as would occur if the base panels were modeled with solid-surface boundary conditions (Fig. 18 of Ref. 6).

The $129 \times 33 \times 33$ grid is rather coarse, being dictated by the available resources of the CRAY X-MP. This coarseness is particularly evident in the wing leading-edge region. An example is shown in Fig. 4, at about 70% semispan. The first 18% of the wing chord is spanned by only three cells of the rectangular grid.

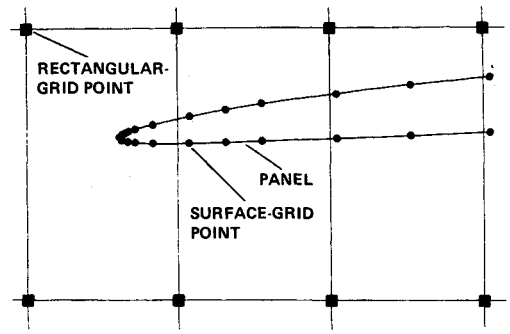

Fig. 4 Detail of leading-edge paneling embedded in the rectangular grid.

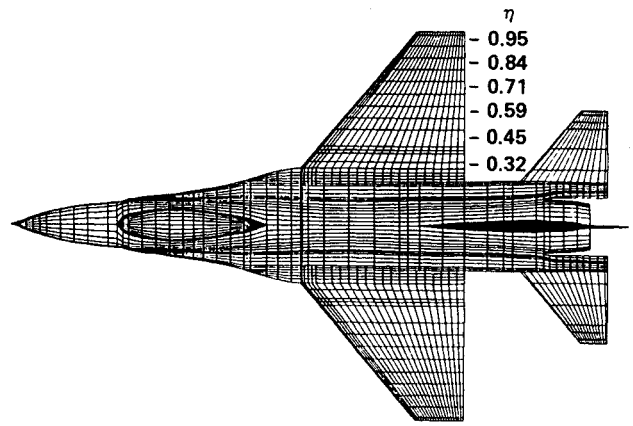

Fig. 5 Wing-pressure stations.

Results

Wing-pressure coefficients from TranAir, PanAir, and wind-tunnel tests are compared at the six wing stations shown in Fig. 5. This is done for $\alpha = 4$ deg, at $M_\infty = 0.6$ and 0.9.

At $M_\infty = 0.6$, the flow is subcritical. Consequently, nonlinear full-potential and linear Prandtl-Glauert solutions should be similar, except in regions where the perturbation velocities are not small compared to the freestream velocity (e.g., near leading-edge stagnation points). Thus, subcritical TranAir results can be assessed by comparing them with results computed with PanAir. These results are shown in Fig. 6, along with wind-tunnel data. The TranAir and PanAir predictions are generally in close agreement, except over the first 5–10% chord, depending on the span station. At $\eta = 32\%$, there are about 33 flowfield grid points along the chord, while at $\eta = 95\%$, this decreases to about 11 points. In this leading-edge region, the rectangular grid density is too sparse to resolve the pressure peaks. Resolution of such rapidly varying behavior, without having to refine the grid everywhere, will require a second-order finite-element basis function for the potential and/or local grid refinement.

At the most outboard station ($\eta = 95\%$), in addition to the large disagreement in the leading-edge region, there is also a smaller disagreement between TranAir and PanAir over the remainder of the chord. The PanAir solution is probably more accurate. This conclusion is based on the predicted velocity components. At the pressure location just upstream of 50% chord, the largest perturbation velocity component predicted by PanAir is the y component on the upper surface, having a magnitude of 19% of the freestream velocity. Hence the small-perturbation assumptions of the linear Prandtl-Glauert equa-

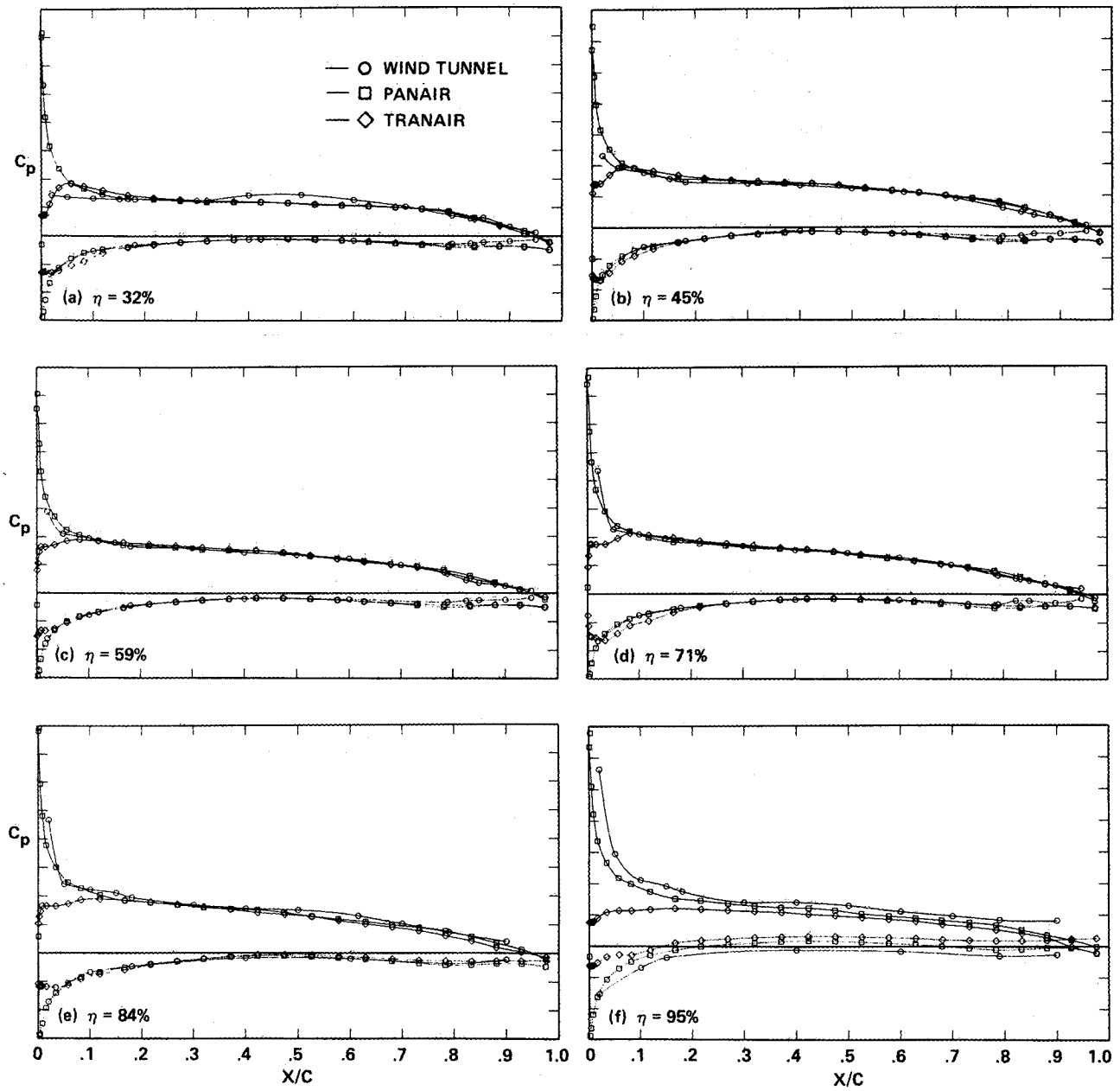

Fig. 6 TranAir results of F-16A; $M_\infty = 0.6$, $\alpha = 4.0$ deg.

tion should be reasonably well satisfied. This is consistent with the fact that the isentropic and second-order pressure coefficient values computed from the PanAir velocities agree within 1%. This suggests that it is the TranAir solution that is least accurate, presumably again caused by the sparse rectangular grid that was used.

The primary discrepancies between the wind-tunnel results and the potential-flow predictions occur at the most inboard and most outboard stations. At the inboard station ($\eta = 32\%$), the experimental data show no leading-edge pressure peak and a slight rise in pressure between about 40 and 60% chord. At the outboard station ($\eta = 95\%$), the experimental data indicate separated flow near the trailing edge. This may be due to the presence of the wingtip missiles and launchers that were present on the wind-tunnel model but not included in the TranAir/PanAir models.

Results for $M_\infty = 0.9$ are shown in Fig. 7. The wind-tunnel data indicate a shock at approximately 75% chord for the four inboard stations. TranAir also indicates a shock, but it is slightly downstream of the shock predicted by the wind tunnel. This result is generally expected from a conservative full-potential solution, because of the absence of a boundary-layer correction (Fig. 40 of Ref. 12) or a correction for entropy conservation at the shock jump. PanAir results, generated to clearly show the difference between a linear- and full-potential solution for a transonic Mach number, do not predict the shock on the aft portion of the wing. The shock predicted by TranAir is smeared over a range of 5–6 grid boxes. Further results have shown that increasing the density of the grid in the x direction greatly reduces the smearing of the shock. As in the $M_\infty = 0.6$ case, TranAir fails to capture the leading-edge pressure peaks. Oil-flow data not presented in this paper indicate that a shock may also exist near the leading edge, from $\eta = 45$ to 84%. At the outboard station ($\eta = 95\%$), TranAir and wind-tunnel results differ greatly. Again, this can probably be attributed to the presence of the tip missile and launcher on the wind-tunnel model that was absent from the TranAir model.

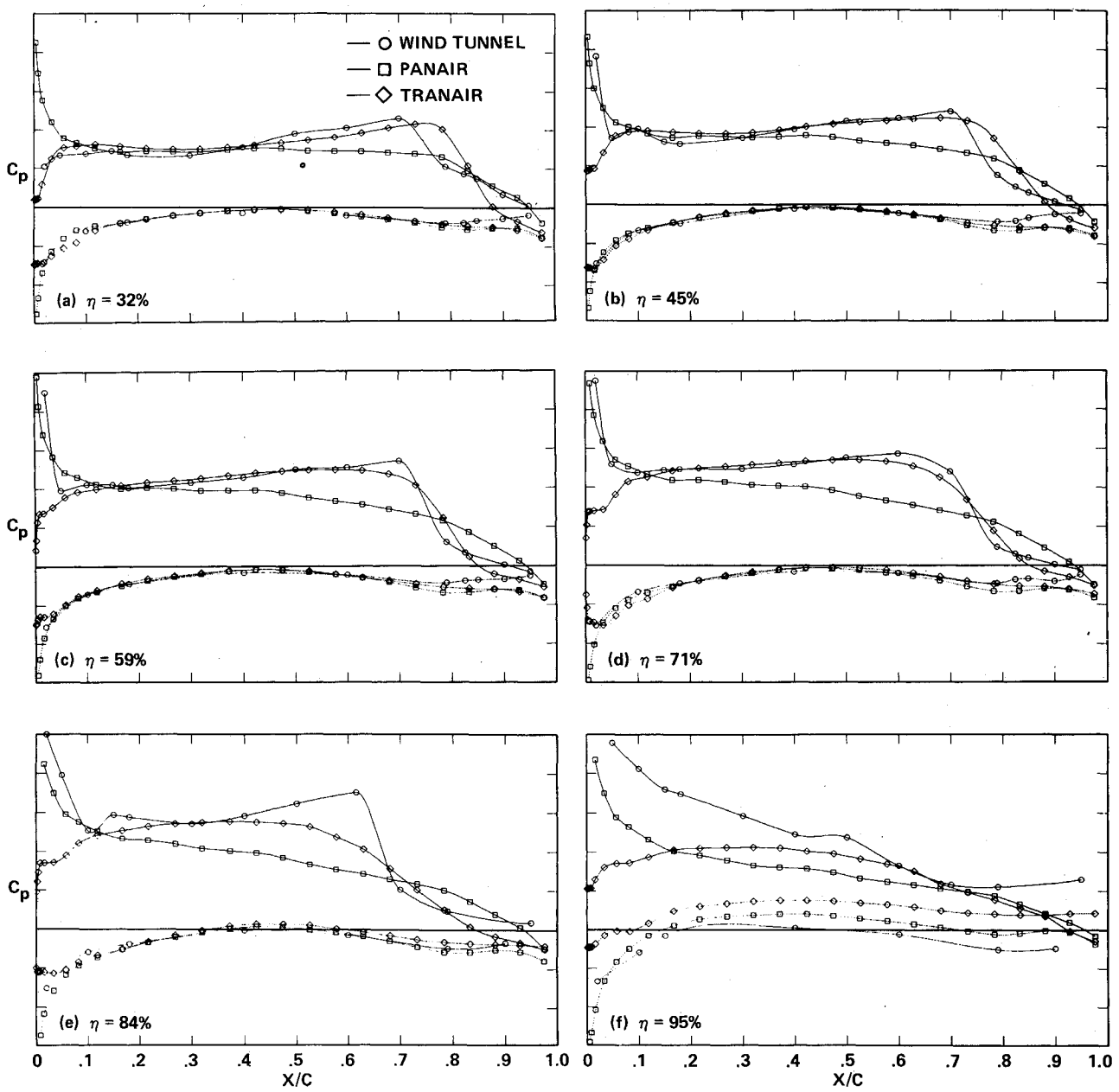

Fig. 7 TranAir results of F-16A; $M_\infty = 0.9$, $\alpha = 4.0$ deg.

TranAir and PanAir results were obtained using a CRAY X-MP/48 with 2-million words of available central memory and a solid-state disk of 16-million words. The PanAir model was run using Boeing's pilot code version of PanAir, since the model contained too many panels to be run with the production code version. For $M_\infty = 0.6$ and 0.9, PanAir used 3485 CPU seconds for each run. To drive the residuals to machine zero, TranAir took 100 iterations and 1700 CPU seconds for the subcritical $M_\infty = 0.6$ case, and 400 iterations and 6000 CPU seconds for the supercritical $M_\infty = 0.9$ case. To obtain five significant digits of accuracy, the $M_\infty = 0.9$ case took 210 iterations and 3000 CPU seconds. Subsequent vectorization improvements have dropped this time to about 1500 s.

Future Plans

The results presented herein are for the first TranAir application to a relatively complete configuration. Studies are needed to determine the solution sensitivity to the number of panels and field grid points. This will be done on the NAS (Numerical Aerodynamic Simulator) CRAY-2 located at NASA Ames Research Center. With an initial memory size of 64-million words of central memory, TranAir models containing up to 25,000 panels and a box of $516 \times 132 \times 68$ grid points should be possible.

Additional F-16A geometry features will be added to the current TranAir model. These include wingtip missiles and launchers, underwing fuel tanks, and the flowthrough nacelle of the wind-tunnel model. Sideslip and deflected leading-edge flap cases are also anticipated.

Refinements currently being made to TranAir include better resolution of rapidly varying flow behavior without increasing the flowfield grid density everywhere. This will be explored using a second-order basis function for the potential, and local grid refinement wherein individual cells of the rectangular grid are subdivided into smaller cells. Efficiency improvements will be made, including a look at multigrid to determine whether it is effective in accelerating the convergence rate. Capability improvements to be explored include the ability to handle supersonic freestream Mach numbers, and the ability to capture wakes separating from sharp leading and trailing edges.

Ultimately, plans include the incorporation of routines to solve the Euler and/or Navier-Stokes equations.

Conclusions

For inviscid flow, the TranAir approach eliminates the need for surface-fitted grids and enables the full geometric generality associated with linear-flow panel methods to be extended to the transonic regime. This has been demonstrated by applying TranAir to the F-16A. The nonlinear full-potential equation is solved for both subcritical and supercritical flow cases and compared with wind-tunnel measurements of wing pressures at $\alpha = 4$ deg.

At $M_\infty = 0.6$, the flow is subcritical and the TranAir results are generally in close agreement with the linear-potential PanAir results, exceptions being in regions of rapidly varying flow such as at the wing leading edge and the wingtip. This is apparently due to locally inadequate flowfield grid density. The PanAir results agree closely with the wind-tunnel results, except near the wingtip ($\eta = 95\%$). The disagreement at the wingtip is presumably because the analytic models do not contain the wingtip missiles and launchers installed on the wind-tunnel model.

At $M_\infty = 0.9$, TranAir captures the shock on the wing. The predicted pressure levels are in fairly close agreement with the wind-tunnel results. For the inboard stations, the predicted shock positions are about 5% chord downstream of the experimental locations. The computed shock sharpness decreases with increasing semispan location. This is probably because the number of flowfield grid points per unit chord decreases with increasing semispan location.

Acknowledgments

The TranAir code is being developed under NASA Contract NAS2-11851. The authors would like to thank F. T. Johnson, J. E. Bussoletti, S. S. Samant, D. P. Young, B. Everson, and R. Burkhart for their work under this contract, and for their invaluable assistance in obtaining the results presented in this paper. The authors also wish to thank K. Li of the University of Illinois for his contributions to the project.

References

[1]Holst, T. L., Slooff, J. W., Yoshihara, H., and Ballhaus, W. F. Jr., "Applied Computational Transonic Aerodynamics," AGARD AG-266, 1982.

[2]Piers, W. J. and Slooff, J. W., "Calculation of Transonic Flow by Means of a Shock-Capturing Field Panel Method," AIAA Paper 79-1459, 1979.

[3]Oskam, B., "Transonic Panel Method for the Full-Potential Equation Applied to Multi-Component Airfoil," *AIAA Journal*, Vol. 23, Sept. 1985, pp. 1327-1334.

[4]Johnson, F. T., James R. M., Bussoletti, J. E., Woo, A. C., and Young, D. P., "A Transonic Rectangular Grid Embedded Panel Method," AIAA Paper 82-0953, 1982.

[5]Erickson, L. L. and Strande, S. M., "A Theoretical Basis for Extending Surface-Paneling Methods to Transonic Flow," *AIAA Journal*, Vol. 23, Dec. 1985, pp. 1860-1867.

[6]Carmichael, R. L. and Erickson, L. L., "PAN AIR—A Higher Order Panel Method for Predicting Subsonic or Supersonic Linear Potential Flows About Arbitrary Configurations," AIAA Paper 81-1255, 1981.

[7]Derbyshire, T. and Sidwell, K. W., "PAN AIR Summary Document (Version 1.0)," NASA CR-3250, 1982.

[8]Magnus, A. E. and Epton, M. A., "PAN AIR—A Computer Program for Predicting Subsonic or Supersonic Linear Potential Flows about Arbitrary Configurations Using a Higher Order Panel Method (Version 1.0), Vol. I, Theory Document," NASA CR-3251, 1981.

[9]Sidwell, K. W., Baruah, P. K., and Busoletti, J. E., "PAN AIR—A Computer Program for Predicting Subsonic or Supersonic Linear Potential Flows About Arbitrary Configurations Using a Higher Order Panel Method (Version 1.0), Vol. II, User's Manual," NASA CR-3252, 1981.

[10]Wigton, L. B., Yu, N. J., and Young, D. P., "GMRES Acceleration of Computational Fluid Dynamics Codes," AIAA Paper 85-1494, 1985.

[11]Rubbert, P. E. et al., "A New Approach to the Solution of Boundary Value Problems Involving Complex Configurations," presented at Symposium on Future Directions of Computational Mechanics, ASME Winter Annual Meeting, Anaheim, CA, Dec. 1986.

[12]Holst, T. L., "Numerical Computation of Transonic Flow Governed by the Full-Potential Equation," NASA TM-84310, 1983.